

ORIGINAL ARTICLES

Impedance analysis of ZnO nanowire coated dry EEG electrodes

Jiamin Wu^{*1}, Wenyan Jia², Chengkun Xu¹, Di Gao¹, Mingui Sun^{2,3}

¹Department of Chemical and Petroleum Engineering, University of Pittsburgh, PA, USA

²Department of Neurosurgery, University of Pittsburgh, PA, USA

³Department of Electrical and Computer Engineering, University of Pittsburgh, PA, USA

Received: September 6, 2016

Accepted: January 2, 2017

Online Published: January 22, 2017

DOI: 10.5430/jbei.v3n1p44

URL: <http://dx.doi.org/10.5430/jbei.v3n1p44>

ABSTRACT

The electrochemical impedance of a novel dry electroencephalogram (EEG) electrode after surface modification (i.e., sputtered with gold, coated with ZnO nanowires) is investigated in this study. To avoid the discomfort caused by repetitive testing on human, a skin-mimic sandwich structure, comprised of a highly porous polyester fabric membrane and two thin silicone films, is fabricated as a test bed. Electrochemical impedance spectroscopy (EIS) measurements are conducted to further understand the properties of the electrode-electrolyte interface when the electrode is installed on this test bed. An equivalent circuit model with a constant phase element (CPE) is used to fit the EIS data. Our results show that the modeled EIS data are in good agreement with the experimental data. It has also been found that the charge transfer resistance decreases from $349 \Omega \text{ cm}^2$ for the bare electrode to $256 \Omega \text{ cm}^2$ for the gold-coated electrode and further decreases to $167 \Omega \text{ cm}^2$ for the gold coated short ZnO nanowire electrode. The lower impedance value will definitely help improve the signal when such electrode is used to record electrophysiological data.

Key Words: Dry EEG electrode, Electrochemical impedance spectroscopy, Nanowires

1. INTRODUCTION

Dry electrode for bio-potential measurement has attracted increasing research attention in recent years. When using such electrode, no skin preparation or gel is required before its installation, which makes long-term biopotential (e.g., EEG) monitoring more comfortable for the patients. In recent years, different types of dry electrodes, such as polymer foam electrode, solid-gel electrode, textile electrode, pin-shaped metallic electrode have been developed.^[1-17] To evaluate the performance of these electrodes, comparing the spontaneous EEG signals (e.g., the alpha wave) or the evoked potential acquired by the dry electrodes and conventional Ag/AgCl electrodes qualitatively or quantitatively is a common approach.^[2-4, 11-13] However, the signal quality

is not only affected by the electrode itself, but also the acquisition components of the EEG system. Electrode-skin contact impedance, therefore, has been used as an indicator to compare the electrode performance. For dry electrodes, usually the impedance is much higher than the wet electrode because no electrolyte is applied at the electrode-skin interface. Coating or processing of the electrode surface has been adopted to lower the impedance and/or improve the biocompatibility. Silver nanowire grown on the surface of polydimethylsiloxane (PDMS) has been demonstrated to form a highly conductive interface.^[14] Titanium/Titanium Nitride or carbon nanotube has also been used to coat electrodes.^[15-17] Electrodes made of silver-coated polymer bristles have been proposed and shown to be more conductive, flexible and comfortable.^[7] Our group has developed a novel dry EEG

*Correspondence: Wenyan Jia; Email: wej6@pitt.edu; Address: Department of Neurosurgery, University of Pittsburgh, PA, USA.

electrode made of stainless steel. It has microteeth around its bottom rim to fix itself on the scalp.^[18,19] We have found that its contact impedance is pretty high, especially at the low frequency region. Then we sputtered gold on the surface of the electrode teeth and observed significant reduced impedance.^[20] However, only two subjects were tested in our previous work. To avoid variance in the impedance measurement caused by individual differences and reduce discomfort of subjects caused by repeated electrode testing, we designed a film to simulate the structure of human skin and used it as a test bed in this work. We also tested the electrode with different coating including gold, and ZnO nanowires. To further investigate the physically meaningful properties of the electrode-skin interface, we used an equivalent circuit model to fit the measured Electrochemical Impedance Spectroscopy (EIS) data.^[21] In this model, a constant phase element (CPE), instead of ideal capacitor, was adopted to simulate the double-layer capacitive behavior of the electrode-skin interface. Our experimental results show that the simulation data using such model are in good agreement with the experimental EIS data.

2. METHODS

2.1 Electrode design and fabrication

The electrode used in this study is called skin screw electrode previously developed by our team.^[18,19] This electrode has a cylinder shape (about 10 mm in diameter), with microteeth around its bottom rim. These teeth help the electrode fix on the surface of the skin after penetrating the top layer of the scalp. So this electrode can be applied and removed very quickly without any requirement of skin preparation or gel/paste. Stainless steel is the material used to make the electrode for good hardness and flexibility (see Figure 1).

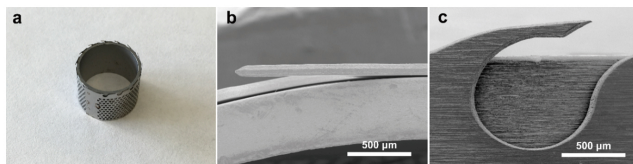


Figure 1. The photograph (a) and top-view (b) and side-view (c) SEM images of a bare screw electrode

2.2 Growth of ZnO nanowire arrays on EEG electrode surface

The schematics of the process of synthesizing ZnO nanowire arrays on EEG electrode is illustrated in Figure 2. The electrodes used in the experiment were carefully checked to make sure that their teeth were intact. The electrodes were cleaned by acetone and ethanol sonication followed by treatment in an UV/ozone cleaner for 15 min. One electrode was selected as reference, without further processing. Two

electrodes were seeded by dip coating with 5 mM zinc acetate solution in ethanol followed by thermal decomposition at 375°C for 20 min. The seeded electrodes were placed in an aqueous growth solution containing 0.025 M zinc nitrate, 0.0125 M hexamethylenetetramine (HMTA), 0.005 M polyethylenimine (PEI), and 0.35 M ammonium hydroxide at 90°C. The as-synthesized ZnO nanowire (NW) array electrodes were then rinsed with deionized water followed by UV/ozone treatment for 15 min. Finally, gold layers (200 nm) were deposited on the bare electrode and ZnO NW array electrodes using magnetron sputtering.

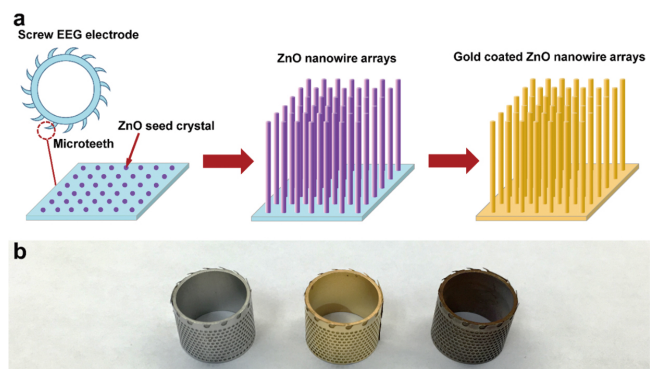


Figure 2. (a) Schematic of the process of preparing ZnO NW coated dry EEG electrodes. (b) Photographs of a bare screw electrode, a gold coated electrode, and a ZnO nanowire coated electrode

2.3 Fabrication of a sandwich structure as test bed

In order to avoid repetitive test on human scalp, an engineered skin-mimic sandwich structure was fabricated to study the scalp-electrode interface impedance. This sandwich structure comprises a highly porous polyester fabric membrane (typically 3 mm thick) sandwiched between two thin silicone films (~200 μm thick). The fabrication process is briefly described as follows. For preparation of the two-part RTV silicone film, 20 g hydroxy-terminated polydimethylsiloxane at a viscosity of 1,800-2,200 cSt, 0.4 g Tris (2-methoxyethoxy)(vinyl) silane, and 0.03 g Dabco® T-12 catalyst were thoroughly mixed for 5 min at room temperature. 15 g of the as-prepared mixture was applied onto two polyethylene terephthalate (PET) sheets (20 cm × 20 cm), and allowed to cure for 2 min. Before the silicone was completely cured, a 20 cm × 20 cm porous polyester fabric membrane was sandwiched between the two coated PET sheets, by bringing two sides of the membrane into contact with the silicone films and applying a moderate pressure to the PET sheets on the top and bottom of the sandwich structure. After the silicone films are completely cured, the two PET sheets were peeled off. The resulted test sandwich structure was stored in PBS buffer at 4°C before testing.

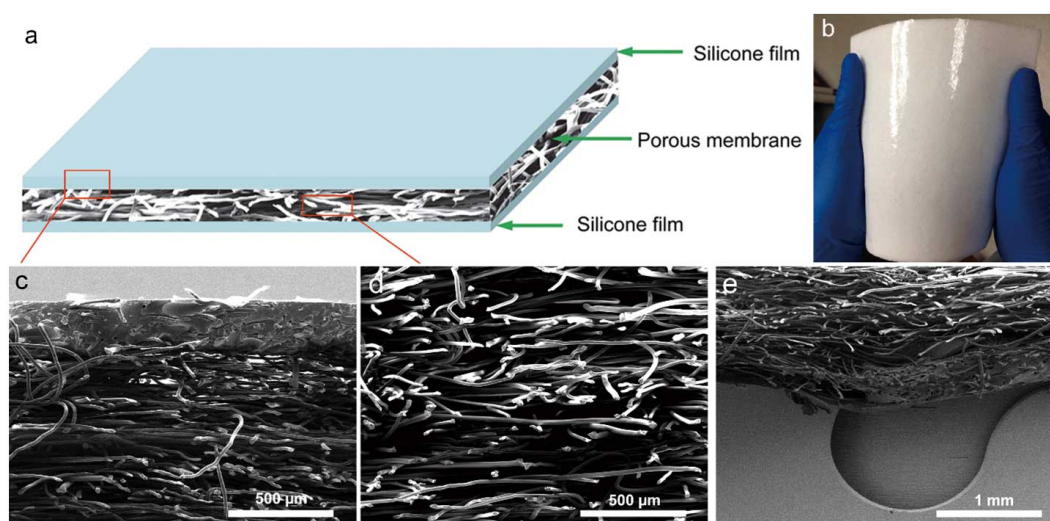


Figure 3. The electrode test sandwich structure to mimics the structure of natural scalp. (a) Schematic illustration of the test structure consists of a highly porous polyester fabric membrane sandwiched between two flexible silicone films ($\sim 200 \mu\text{m}$ thickness). (b) Photograph of this electrode test sandwich structure. (c) Cross-section SEM image of the top silicone film. (d) Cross-section SEM image of the middle porous polyester membrane in the test sandwich structure. (e) SEM image of one tooth of the electrode penetrating into the test structure

Figure 3a shows schematic illustration of the test structure consisting of a highly porous polyester fabric membrane sandwiched between two flexible silicone films ($\sim 200 \mu\text{m}$ thickness each as shown in Figure 3c). The polyester fabric membrane as a scaffold had an interconnected pore structure with average pore size of $50 \mu\text{m}$ (see Figure 3d), which is also used to retain the buffer solution, whereas the silicone films are used to seal the buffer solution and provide mechanical support for anchoring the electrode. The cross-sectional SEM image (see Figure 3e) could confirm reliable and reproducible penetration of microteeth on the EEG electrode across the silicone film into the porous membrane during the placement of EEG electrodes.

2.4 Electrochemical impedance spectroscopy measurement

The electrochemical impedance spectroscopy measurements were performed in the above sandwich structure by using a potentiostat (Gamry Reference 600), connected to a three-electrode setup consisting of the sample as the working electrode (WE), a platinum wire as the counter electrode (RE), and a solid-state Ag/AgCl reference electrode (see Figure 4). The solid-state Ag/AgCl reference electrode was obtained by chemical oxidation of a polished Ag wire in 0.1 M FeCl₃ solution for 60 s at room temperature. Potentiostatic EIS tests were carried out at open circuit potential with ac perturbation amplitude of 5 mV in the frequency range from 0.1 Hz to 100 KHz. The obtained impedance data were analyzed by ZSimpWin software and fitted to the appropriate equivalent circuit models. In order to test the reproducibility of the

results, the experiments were performed ten times. For each test the electrodes were placed in different positions of the electrode test sandwich structure, while the distance between WE and CE was kept at 5 cm and RE was 3 mm away from WE.

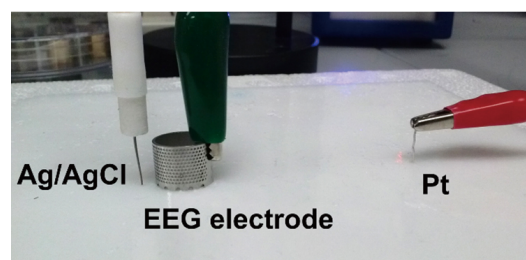


Figure 4. Three-electrode setup for EIS measurement and electrode location

2.5 Electrochemical impedance spectroscopy analysis

Electrochemical impedance spectroscopy analysis is a powerful tool in evaluating the electrode-skin interface. Several electrical circuit models have been proposed to fit the EIS data, such as Warburg model, Fricke model, Randles circuit model, Geddes and Baker model.^[21–23] The simplified Randles model (see Figure 5a), which is the most commonly used one, includes a resistance of the electrolyte solution R_s , and a double layer capacitor C_{dl} in parallel with a charge transfer resistance R_{ct} . The two parallel components account for the non-Faradic and Faradic processes, respectively. A more complicated Randles model with mixed kinetic and charge-transfer control was also proposed (see Figure 5b). In

this model, the impedance of the Faradaic reaction consists of a charge transfer resistance R_{ct} and a specific electrochemical element of diffusion W , called Warburg element. The Warburg impedance (W) is resulted from diffusion of ions from bulk electrolyte to electrode surface, and defined as

$$W = \frac{1}{Y_W \sqrt{j\omega}} \quad (1)$$

where Y_W is the Warburg coefficient, j is the imaginary unit, ω is the angular frequency. Later, a CPE describing the double layer capacitance has been used to replace the pure capacitance C_{dl} .^[24] It reflects the characteristics of a micro-

scopic fractal at blocking electrode-skin interfaces. CPE is defined as

$$CPE = \frac{1}{Y_0(j\omega)^n} \quad (2)$$

where Y_0 is the measured magnitude of CPE, n is a parameter between 0 and 1. For a perfect capacitor, $n = 1$; while in the case of $n = 0$, the impedance represents a resistor. The value of n reveals the micro structure of the interface. It can be affected by the roughness, and other inhomogeneities or relaxation processes of the electrode surface.

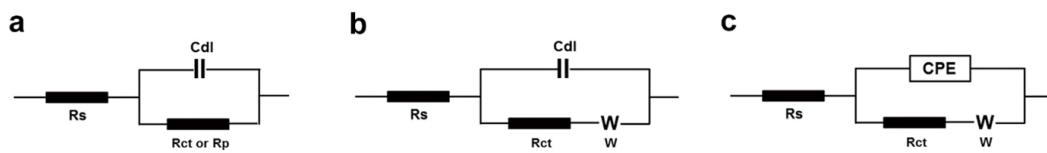


Figure 5. Equivalent circuits proposed for analyzing the EIS profiles

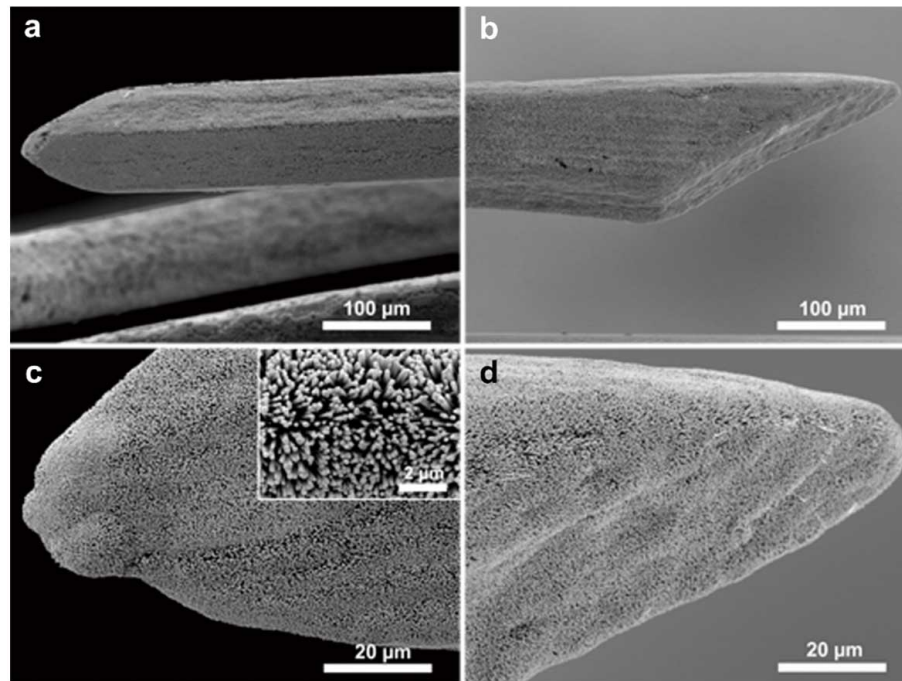


Figure 6. Top-view (a, b) and side-view (c, d) SEM images of ZnO NW arrays grown for 1 h on the electrode. The insert shows a high magnification SEM image

3. RESULTS AND DISCUSSION

3.1 ZnO nanowires coated EEG electrodes

The SEM images of the fabricated ZnO nanowire coated EEG electrodes are shown in Figure 6. As observed from the figures, well aligned ZnO NWs uniformly covered the surface of electrode with a wire density of about 8×10^7

wires/cm². Each wire is approximately 150-200 nm in diameter.

3.2 Electrochemical impedance spectroscopy

The electrochemical impedance spectroscopy measurements were carried out with electrodes in our fabricated test sand-

wich structure, which mimics the natural structure of human skin. The Bode plots of EIS of the bare electrode, gold-coated electrode, and gold-coated ZnO NWs electrodes are shown in Figure 7a. It can be seen that the impedance of the gold-coated electrode is much lower than the uncoated bare

electrode and the impedances of both gold coated ZnO NWs electrodes are lower than those of the bare and gold-coated electrodes at low and medium frequencies. However, the difference between the two gold-coated ZnO NWs electrodes with different NW lengths is not significant.

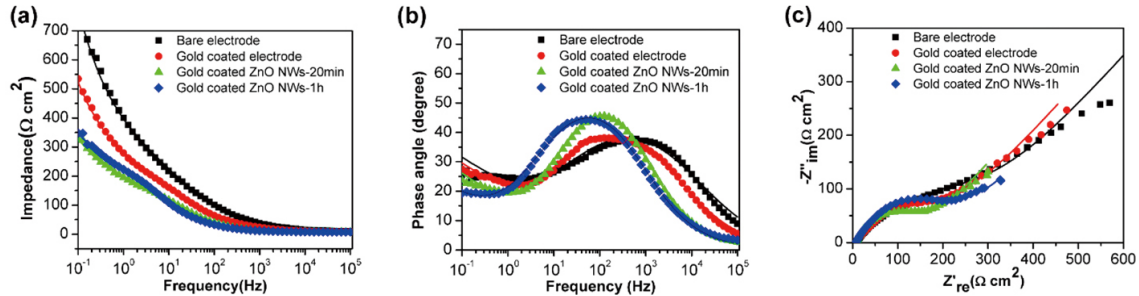


Figure 7. Electrochemical impedance spectroscopy for bare electrode, gold-coated electrode, and gold-coated ZnO NW electrodes. (a) Bode magnitude, (b) Bode phase, and (c) Nyquist plots. Solid lines are fitting curves to the equivalent circuit in Figure 5c.

There was a common feature for all Nyquist curves (see Figure 7c), a distorted capacitive arc in the high- and medium-frequency region followed by a straight line with a slope close to 45° in the low frequency region. The electrical circuit model shown in Figure 5c is used to fit the impedance data and the fitting parameters for all equivalent circuit ele-

ments are summarized in Table 1. In the present fitting, all χ^2 values within the order of 10^{-3} and the error percentages corresponding to each component of the equivalent circuit less than 5% indicate a good fitting with the proposed equivalent circuits.

Table 1. Electrochemical parameters for the equivalent circuit elements obtained by fitting experimental impedance data in Figure 7

Sample	R_s ($\Omega \text{ cm}^2$)	CPE		R_{ct} ($\Omega \text{ cm}^2$)	Y_w ($\text{S s}^{0.5} \text{ cm}^{-2}$)
		Y_0 ($\text{S s}^n \text{ cm}^{-2}$)	n		
Bare	8.06 ± 0.89	$(2.43 \pm 0.36) \times 10^{-4}$	0.55 ± 0.06	349 ± 41	$(2.10 \pm 0.39) \times 10^{-3}$
Gold-coated	7.84 ± 0.61	$(3.19 \pm 0.15) \times 10^{-4}$	0.59 ± 0.03	256 ± 20	$(3.42 \pm 0.26) \times 10^{-3}$
Gold-coated ZnO NWs-20 min	6.97 ± 0.52	$(2.48 \pm 0.19) \times 10^{-4}$	0.72 ± 0.04	167 ± 18	$(6.33 \pm 0.45) \times 10^{-3}$
Gold-coated ZnO NWs-1 h	7.29 ± 0.72	$(3.03 \pm 0.31) \times 10^{-4}$	0.69 ± 0.07	228 ± 35	$(7.97 \pm 0.75) \times 10^{-3}$

It has been found that the charge transfer resistance (R_{ct}) decreases from its initial value of $349 \Omega \text{ cm}^2$ for the bare electrode to $256 \Omega \text{ cm}^2$ for the gold-coated electrode and further decreases to $167 \Omega \text{ cm}^2$ for the gold-coated short ZnO NWs electrode. This indicates that the decoration of the bare electrode surface with ZnO NW arrays facilitates electrolyte ions transfer from the solution to the electrode. In general, the rough and porous structured electrode would effectively accelerate electrolyte diffusion and charge transfer.^[25] However, R_{ct} increased from $167 \Omega \text{ cm}^2$ to $228 \Omega \text{ cm}^2$ as increasing the length of the ZnO NW arrays due to the poorer accessibility of the ions to the electrode. The high-density long semiconducting ZnO NW arrays on the electrode can cause the charge transfer rate slow down. The values of n in CPE of these EEG electrodes have also a

significant deviation from the pure capacitive behavior of the electrodes due to the high surface heterogeneity.

We have also conducted the impedance spectroscopy on two human subjects under the approval of the Institutional Review Board (IRB) at the University of Pittsburgh. Two electrodes (i.e., a bare electrode and a gold-coated electrode) were placed side-by-side on the scalp at two different locations (no hair site F3, and hair site C3). The ZnO NWs electrode was not tested due to the potential concerns about its biocompatibility. A conventional EEG disc electrode was placed on the forehead as the counter electrode. No skin preparation was conducted for all these electrodes. The impedance data were collected in the frequency range between 1 and 10 KHz at 5 mV RMS. Figure 8 shows a typical Bode magnitude plot for one subject. The impedances of the

bare and gold-coated electrodes show similar trends as in the previous experiment with our test bed, with a much lower impedance for the gold-coated electrode.

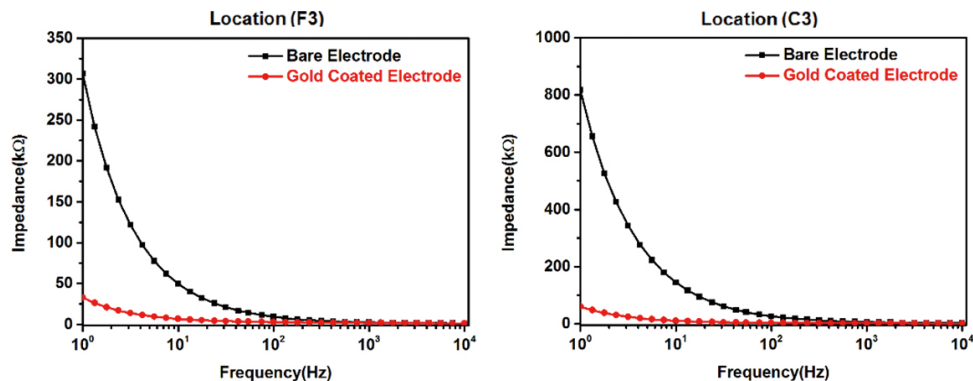


Figure 8. Bode magnitude for bare electrode, gold-coated electrode, and disc electrode installed on human scalp

4. CONCLUSION

A novel screw dry electrode has been developed for EEG measurements, on which ZnO nanowire arrays with diameters in the range of 100-200 nm are synthesized via a simple wet chemical method. The nanowires are well-aligned and strongly attached to the microteeth of the electrode. A sandwich structure testing platform, designed to mimic structures of scalp skin, was successfully fabricated to serve as an efficient and cost-effective alternative to the human testing to study the skin-electrode interface impedance. The electrochemical impedance spectra show that the short

ZnO nanowire coated electrode provide lower electrode-skin impedance due to large surface areas and excellent charge transfer compared to the bare electrode and gold coated electrode. The developed dry electrode prototype can be readily applicable to high quality EEG measurements without any uncomfortable preparation for clinical and research applications.

ACKNOWLEDGEMENTS

This work was supported by National Institutes of Health grants R01EB013174, U54EB007954, and Point-of-Care Center for Emerging Neuro-Technologies (POC-CENT).

REFERENCES

- [1] Lopez-Gordo MA, Sanchez-Morillo D, Valle FP. Dry EEG electrodes. *Sensors*. 2014; 14(7): 12847-70. PMID:25046013. <https://doi.org/10.3390/s140712847>
- [2] Chi YM, Jung TP, Cauwenberghs G. Dry-contact and noncontact biopotential electrodes: methodological review. *IEEE Rev Biomed Eng*. 2010; 3: 106-19. <http://www.ncbi.nlm.nih.gov/pubmed/22275204>
- [3] Huang YJ, Wu CY, Wong AMK, et al. Novel active comb-shaped dry electrode for EEG measurement in hairy site. *IEEE Trans Biomed Eng*. 2015; 62(1): 256-63. PMID:25137719. <https://doi.org/10.1109/TBME.2014.2347318>
- [4] Lofhede J, Seoane F, Thordstein M. Textile electrodes for EEG recording - a pilot study. *Sensors*. 2012; 12(12): 16907-19. PMID:23223149. <https://doi.org/10.3390/s121216907>
- [5] Baek HJ, Lee HJ, Lim YG, et al. Conductive polymer foam surface improves the performance of a capacitive EEG electrode. *IEEE Trans Biomed Eng*. 2012; 59(12): 3422-31. <http://www.ncbi.nlm.nih.gov/pubmed/22961261>
- [6] Toyama S, Takano K, Kansaku K. A non-adhesive solid-gel electrode for a non-invasive brain-machine interface. *Front Neurol*. 2012; 3: 114. PMID:22826701.
- [7] Grozea C, Voinescu CD, Fazli S. Bristle-sensors-low-cost flexible passive dry EEG electrodes for neurofeedback and BCI applications. *J Neural Eng*. 2011; 8(2): 8.
- [8] Fiedler P, Pedrosa P, Griebel S, et al. Novel flexible dry PU/TiN-multipin electrodes: first application in EEG measurements. in *Proc. IEEE Annual Conference of the Engineering in Medicine and Biology Society*; 2011. pp. 55-8.
- [9] Liao LD, Wang IJ, Chen SF, et al. Design, fabrication and experimental validation of a novel dry-contact sensor for measuring electroencephalography signals without skin preparation. *Sensors*. 2011; 11(6): 5819-34. PMID:22163929. <https://doi.org/10.3390/s110605819>
- [10] Salvo P, Raedt R, Carrette E, et al. A 3D printed dry electrode for ECG/EEG recording. *Sensors and Actuators a-Physical*. 2012; 174: 96-102. <https://doi.org/10.1016/j.sna.2011.12.017>
- [11] Wang L, Liu J, Yang B, et al. PDMS-based low cost flexible dry electrode for long-term EEG measurement. *IEEE Sensors J*. 2012; 12(9): 2898-904.
- [12] Lin CT, Liao LD, Liu YH, et al. Novel dry polymer foam electrodes for long-term EEG measurement. *IEEE Trans Biomed Eng*. 2011; 58(5): 1200-7. PMID:21193371. <https://doi.org/10.1109/TBME.2010.2102353>

- [13] Grummett TS, Leibbrandt RE, Lewis TW, et al. Measurement of neural signals from inexpensive, wireless and dry EEG systems. *Physiol Meas.* 2015; 36(7): 1469-84. PMID:26020164. <https://doi.org/10.1088/0967-3334/36/7/1469>
- [14] Myers AC, Huang H, Zhu Y. Wearable silver nanowire dry electrodes for electrophysiological sensing. *Rsc Advances.* 2015; 5(15): 11627-32. <https://doi.org/10.1039/C4RA15101A>
- [15] Ruffini G, Dunne S, Farres E, et al. ENOBIO dry electrophysiology electrode; first human trial plus wireless electrode system. in *Proc. IEEE Annual Conference of the Engineering in Medicine and Biology Society*; 2007. pp. 6690-4.
- [16] Fiedler P, Fonseca C, Pedrosa P, et al. Novel flexible dry multipin electrodes for EEG: Signal quality and interfacial impedance of Ti and TiN coatings. in *Proc. IEEE Annual Conference of the Engineering in Medicine and Biology Society*; 2013. pp. 547-50
- [17] Pedrosa P, Alves E, Barradas NP, et al. TiNx coated polycarbonate for bio-electrode applications. *Corrosion Science.* 2012; 56: 49-57. <https://doi.org/10.1016/j.corsci.2011.11.008>
- [18] Sun M, Jia W, Liang W, et al. A low-impedance, skin-grabbing, and gel-free EEG electrode. in *Proc. 34th Annual International Conference of the IEEE Engineering in Medicine and Biology Society*; 2012 August 28- September 1; San Diego, CA. pp. 1992-5. Available from: <http://www.ncbi.nlm.nih.gov/pubmed/23366308>
- [19] Sun M, Sciabassi RJ, Liang W, et al. Skin screw electrode U.S. patent US 12/012,607. Issue Date: Feb. 7, 2012.
- [20] Jia W, Wu J, Gao D, et al. Characteristics of skin-electrode impedance for a novel screw electrode. in *Proc. IEEE Annual Northeast Bioengineering Conference*; 2014. pp. 1-2.
- [21] Barsoukov E, Macdonald JR, editors. *Impedance spectroscopy: theory, experiment, and applications.* 2nd ed. Hoboken, New Jersey: John Wiley & Sons, Inc.; 2005.
- [22] Geddes LA. Historical evolution of circuit models for the electrode-electrolyte interface. *Annals of Biomedical Engineering.* 1997; 25(1): 1-14. <https://doi.org/10.1007/BF02738534>
- [23] McAdams ET, Jossinet J. Tissue impedance: a historical overview. *Physiol Meas.* 1995; 16(3 Suppl A): A1-13. Available from: <http://www.ncbi.nlm.nih.gov/pubmed/8528108>
- [24] Mcadams ET, Lacknermeier A, McLaughlin JA, et al. The Linear and nonlinear electrical-properties of the electrode-electrolyte interface. *Biosensors & Bioelectronics.* 1995; 10(1-2): 67-74.
- [25] Wang Y, Zhu Y, Chen J, et al. Amperometric biosensor based on 3D ordered freestanding porous Pt nanowire array electrode. *Nanoscale.* 2012; 4(19): 6025-31. <http://dx.doi.org/10.1039/C2NR31256E>